# Influence of Flanking Residues on Tilt and Rotation Angles of Transmembrane Peptides in Lipid Bilayers. A Solid-State 2 H NMR Study

**4 AUTHORS**, INCLUDING:

Rob M J Liskamp
University of Glasgow
**413** PUBLICATIONS **11,083** CITATIONS

SEE PROFILE

Josephine Antoinette Killian
Utrecht University
**166** PUBLICATIONS **8,635** CITATIONS

SEE PROFILE

# Influence of Flanking Residues on Tilt and Rotation Angles of Transmembrane Peptides in Lipid Bilayers. A Solid-State $^2$H NMR Study

Suat Özdirekcan,*,‡ Dirk T. S. Rijkers,§ Rob M. J. Liskamp,§ and J. Antoinette Killian‡

*Department of Biochemistry of Membranes, Bijvoet Center for Biomolecular Research, Utrecht University, Padualaan 8, 3584 CH Utrecht, The Netherlands, and Department of Medicinal Chemistry, Utrecht Institute for Pharmaceutical Sciences, Faculty of Pharmaceutical Sciences, Utrecht University, Sorbonnelaan 16, 3584 CA Utrecht, The Netherlands*

ABSTRACT: To gain insight into the parameters that determine the arrangement of proteins in membranes, $^2$H NMR experiments were performed to analyze tilt and rotation angles of membrane-spanning α-helical model peptides upon incorporation in diacylphosphatidylcholine bilayers with varying thickness. The peptides consisted of the sequence acetyl-GW$_2$(LA)$_8$LW$_2$A-NH$_2$ (WALP23) and analogues thereof, in which the interfacial Trp residues were replaced by Lys (KALP23) and/or the hydrophobic sequence was replaced by Leu (WLP23 and KLP23). The peptides were synthesized with a single deuterium-labeled alanine at four different positions along the hydrophobic segment. For all peptides a small but systematic increase in tilt angle was observed upon decreasing the bilayer thickness. However, significantly larger tilt angles were obtained for the Lys-flanked KALP23 than for the Trp-flanked WALP23, suggesting that interfacial anchoring interactions of Trp may inhibit tilting. Increasing the hydrophobicity resulted in an increase in tilt angle for the Trp-flanked analogue only. For all peptides the maximum tilt angle obtained was remarkably small (less than 12°), suggesting that further tilting is inhibited, most likely due to unfavorable packing of lipids around a tilted helix. The results furthermore showed that the direction of tilt is determined almost exclusively by the flanking residues: Trp- and Lys-flanked peptides were found to have very different rotation angles, which were influenced significantly neither by hydrophobicity of the peptides nor by the extent of hydrophobic mismatch. Finally, very small changes in the side chain angles of the deuterated alanine probes were observed in Trp-flanked peptides, suggesting that these peptides may decrease their hydrophobic length to help them to adapt to thin membranes.

Membrane proteins carry out many essential functions in cells. In the specific case of integral proteins, the membrane spanning parts of these molecules are in direct contact with acyl chains and headgroups of the surrounding lipids. Consequently, the lipid environment can modulate structure and dynamics and, hence, activity of membrane proteins (*1*). For example, changes in hydrophobic thickness of a lipid bilayer can affect the structure of an integral membrane protein by causing a hydrophobic mismatch between the bilayer thickness and the length of the membrane spanning parts of that protein (reviewed in refs *2−4*). Understanding the molecular basis of how lipids influence membrane proteins requires precise information on structural properties of transmembrane segments of proteins and knowledge of how these properties are sensitive to protein and lipid composition. It is most suitable to perform such experiments on model membranes of synthetic lipids and transmembrane peptides, since the composition of both the lipids and the peptides can be systematically varied. Model membranes,

made of phosphatidylcholine derivatives (PC)[1] and model transmembrane peptides, have already been extensively studied to investigate the effects of hydrophobic mismatch on lipid−peptide interactions (*5−15*; reviewed in refs *2−4*). In particular, the so-called WALP peptides have been used as tools to monitor the consequence of hydrophobic mismatch for the organization of peptides and lipids in model membranes (reviewed in ref *15*). WALP peptides are a family of α-helical transmembrane model peptides made of a central leucine alanine stretch that is flanked by two tryptophan residues on each side.

Recently, a technique based on solid-state $^2$H NMR using deuterated alanines has been developed to analyze structural properties of transmembrane peptides in model membranes (*10, 11, 14, 16*). This method, called geometric analysis of labeled alanines (GALA), allows for very accurate determination of tilt angles of WALP peptides in either oriented or nonoriented PC bilayers (*11, 14*). In addition, the direction in which the peptides are tilted, as determined by their

* Corresponding author. E-mail: s.ozdirekcan@chem.uu.nl. Phone: +31-30-2533853. Fax: +31-30-2533969.
‡ Department of Biochemistry of Membranes, Bijvoet Center for Biomolecular Research, Utrecht University.
§ Department of Medicinal Chemistry, Utrecht Institute for Pharmaceutical Sciences, Faculty of Pharmaceutical Sciences, Utrecht University.

[1] Abbreviations: PC, phosphatidylcholine; NMR, nuclear magnetic resonance; TFA, trifluoroacetic acid; TFE, 2,2,2-trifluoroethanol; HEPES, *N*-(2-hydroxyethyl)piperazine-*N*′-2-ethanesulfonic acid; tBu, *tert*-butyl; $d_4$-Ala, deuterated L-alanine-$d_4$; Fmoc, 9-fluorenylmethyloxycarbonyl; di-C12:0-PC, 1,2-dilauroyl-*sn*-glycero-3-phosphocholine; di-C13:0-PC, 1,2-ditridecanoyl-*sn*-glycero-3-phosphocholine; di-C14:0-PC, 1,2-dimyristoyl-*sn*-glycero-3-phosphocholine; di-C18:1-PC, 1,2-dioleoyl-*sn*-glycero-3-phosphocholine.

Table 1:  Amino Acid Sequences of the Peptides Used

| peptide | design |
|---|---|
| Ac-WALP23-$d_4$-Ala-NH$_2$ | Ac-GWWL**A**L**A**LALALAL**A**L**A**LALALWWA-NH$_2$[a] |
| Ac-KALP23-$d_4$-Ala-NH$_2$ | Ac-GKKL**A**L**A**LALALAL**A**L**A**LALALKKA-NH$_2$[a] |
| Ac-WLP23-$d_4$-Ala-NH$_2$ | Ac-GWWLLLLLLL**LLLLL**LLLLLLWWA-NH$_2$[b] |
| Ac-KLP23-$d_4$-Ala-NH$_2$ | Ac-GKKLLLLLLL**LLLL**LLLLLLKKA-NH$_2$ |

[a] Underlined letters indicated in bold are positions where the peptides have been labeled with $d_4$-Ala. [b] Underlined bold characters indicate the residues that have been replaced by $d_4$-Ala for single labeling. If not deuterium labeled, leucine residues occupied those positions.

rotation angles, can be analyzed with this method. Previous results (*14*) showed that when the hydrophobic length of WALP peptides exceeds the bilayer thickness (i.e., under conditions of positive hydrophobic mismatch), the peptides are more tilted in the thinnest bilayers with a preferential rotation angle that is independent of mismatch. However, the tilt angles were much too small to compensate for hydrophobic mismatch, suggesting that tilting is also affected by parameters other than the hydrophobic thickness of the membrane. One such parameter is likely to be the amino acid composition of the peptides. For instance, aromatic residues are thought to have a preference for the lipid−water interface in PC bilayers (*4, 17, 18*), and therefore, the flanking tryptophan residues in WALP peptides could influence the way that these peptides are positioned in the membrane. In addition, other features such as hydrophobicity of the peptide might play a part in this process. To gain insight into the role of amino acid composition in determining the arrangement of peptides in membranes, we performed in the present study $^2$H NMR experiments on transmembrane model peptides of different composition in unoriented PC bilayers, using an approach similar to that in Strandberg et al. (*14*). All experiments were conducted in PC bilayers with varying acyl chain length in their liquid-crystalline phase. Comparison of the mismatch-dependent behavior of Trp- and Lys-flanked transmembrane peptides showed that, besides hydrophobic mismatch, flanking residues play an important role in determining both the tilt and rotation angles of the peptides. In contrast, hydrophobicity of the transmembrane part seemed to have at most a small effect on the arrangement of the different peptides in the lipid bilayer. Finally, small changes in the side chain angles of the deuterated alanine probes in the helix suggest that, in contrast to their Lys-flanked counterparts, Trp-flanked peptides may slightly decrease their hydrophobic length to help them to adapt to the thinnest lipid bilayers.

## MATERIALS AND METHODS

### Materials

WALP23, KALP23, WLP23, and KLP23 (for amino acid sequence, see Table 1) were synthesized using Fmoc/tBu solid-phase peptide synthesis as described elsewhere for related KALP peptides (*19*). Deuterated L-alanine-$d_4$ was obtained from Sigma Aldrich, and 9-fluorenylmethyloxy-carbonyl (Fmoc) was used to protect its amino functionality as described by Ten Kortenaar et al. (*20*) before being used in the synthesis. The peptides were isotopically labeled with one deuterium-labeled alanine residue at different positions in the transmembrane domain. 1,2-Dilauroyl-*sn*-glycero-3-phosphocholine (di-C12:0-PC), 1,2-ditridecanoyl-*sn*-glycero-3-phospholcholine (di-C13:0-PC), 1,2-dimyristoyl-*sn*-glycero-

3-phosphocholine (di-C14:0-PC), and 1,2-dioleoyl-*sn*-glycero-3-phosphocholine (di-C18:1-PC) were purchased from Avanti Polar Lipids Inc. (Alabaster, AL) and used without further purification. Trifluoroacetic acid (TFA) and 2,2,2-trifluoro-ethanol (TFE) were obtained from Merck (Darmstadt, Germany). Deuterium-depleted water was obtained from Cambridge Isotope Laboratories, Inc. All other chemicals were of analytical grade. Water was deionized and filtered with a Milli-Q Water purification system from Millipore (Bedford, MA).

### Methods

*NMR Sample Preparation.* Stock solutions were prepared of ca. 10 mM phospholipid in chloroform, and the exact concentrations of the phospholipid stocks were determined by a phosphorus assay (*21*). For each sample 1 $\mu$mol of peptide was used, which was dissolved in 1 mL of TFE and dried to a film in a rotavapor twice in order to remove residual traces of TFA. Subsequently, the peptide film was dissolved in 1 mL of TFE and added to a lipid solution containing 100 $\mu$mol of phospholipid to achieve a peptide to lipid molar ratio of 1/100. The mixture was vortexed and dried to a film in a rotavapor. Traces of solvent in samples were further evaporated overnight under vacuum (ca. 1 × 10$^{-2}$ bar).

The lipid−peptide films were hydrated in either 100 $\mu$L of deuterium-depleted water for WALP23 samples or deuterium-depleted buffer for KALP23 samples (25 mM HEPES, 100 mM NaCl, pH 7.4), and the suspension was transferred to 7 mm diameter glass tubes. Control experiments with KALP23 samples were performed with and without buffer to show that the buffer does not affect the $^2$H NMR signal (data not shown). The peptide/lipid suspensions did not affect the pH of either the buffer or the water that was used for hydration. The tubes were sealed under a N$_2$ atmosphere with a silicon stopper and epoxy glue. Samples were freeze−thawed at least 10 times to promote sample homogeneity.

*NMR Measurements.* NMR experiments were carried out on a Bruker Avance 500 MHz NMR spectrometer. Unless stated otherwise, measurements were performed at 40 °C. Samples were allowed to equilibrate at this temperature for at least 10 min before measurements.

$^{31}$P NMR experiments were performed as described (*14*) on all samples used. In all cases the spectra were similar to those reported previously for WALP/DMPC samples (*6*), confirming a bilayer organization of the lipids (data not shown).

$^2$H NMR experiments were performed at 76.78 MHz using a quadrupolar echo sequence as described previously (*14*).

*Calculations.* Quadrupolar splittings from the labeled positions were measured from $^2$H NMR spectra. As in
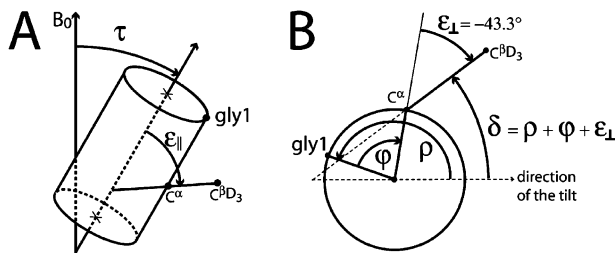
FIGURE 1: Definition of angles used in the calculations. (A) The tilt angle $\tau$ between the peptide axis and the bilayer normal, which is assumed to be along the magnetic field direction. The bond angle between the C−CD$_3$ bond and the peptide axis is denoted by $\epsilon_{\parallel}$. (B) The rotation angle giving the orientation of the C−CD$_3$ bond is indicated as $\delta$. The angle $\delta$ is determined by three contributions that are $\rho$, $\varphi$, and $\epsilon_{\perp}$. $\rho$ is the rotation of the whole peptide, and it is defined as the anticlockwise rotation angle of C$^{\alpha}$ of Gly1, compared to the direction of the tilt (reference position). $\varphi$ is the angle by which another amino acid residue is rotated around the peptide axis with respect to Gly1. $\epsilon_{\perp}$ is the angle of the C$^{\alpha}$−CD$_3$ bond projected onto a plane perpendicular to the helical axis with respect to a vector (or line) between the peptide axis and the C$^{\alpha}$. (Angles in the figure are chosen arbitrarily for clarity.)

previous work (*11*), the splitting of the backbone deuteron could not be observed, and the $^2$H NMR signals were assigned to the deuterons of the alanine side chain methyl group. The data were fitted to a model α-helix, similar to that in previous studies (*10, 11, 14, 16*). In particular, data were fitted to the equation

$$\Delta\nu_q = \tfrac{1}{2}\{(3/4)K(3\cos^2\epsilon_{\parallel}(\cos\tau - \sin\tau\cos\delta\tan\epsilon_{\parallel})^2 - 1)\} \quad (1)$$

$\Delta\nu_q$ is the quadrupolar splitting as measured in unoriented samples. $K$ is a constant with a frequency dimension. The angles $\tau$, $\epsilon_{\parallel}$, and $\delta$ depend on the peptide geometry and orientation (Figure 1). The tilt angle denoted $\tau$ is defined as the angle between the peptide helical axis and the bilayer normal, and $\epsilon_{\parallel}$ is the angle between the peptide helix axis and the C$^{\alpha}$−C$^{\beta}$D$_3$ bond vector (Figure 1A). $\delta$ is the rotation angle of the labeled bond vector around the helical axis with respect to the direction of the tilt (Figure 1B). As depicted in Figure 1B, three angles are contributing to $\delta$:

$$\delta = \rho + \epsilon_{\perp} + \varphi \quad (2)$$

where $\rho$ is the rotation around the helical axis of the C$^{\alpha}$ of Gly1 with respect to the direction of the tilt, $\epsilon_{\perp}$ is the angle of the bond vector C$^{\alpha}$−C$^{\beta}$D$_3$ with respect to a vector from C$^{\alpha}$ to the peptide axis, and $\varphi$ is the pitch (or rotation) angle between both C$^{\alpha}$ of the reference Gly1 and C$^{\alpha}$ of the labeled residue in the peptide. For a regular helix

$$\varphi = -(n-1)\psi \quad (3)$$

where $n$ is the residue number and $\psi$ is the pitch angle between two neighboring residues. In an ideal α-helix $\psi = 100°$. The value of $\epsilon_{\perp}$, which has been estimated from molecular models using the insight II database, was kept constant at $-43.3°$ for all calculations (see also ref *11*). $\tau$ and $\rho$ were used as the fitting parameters in the calculations, and $\epsilon_{\parallel}$ was allowed to vary in a range between 51° and 64° based on modeling of typical transmembrane α-helical structures (see below). The constant $K$ is defined as

$$K = (e^2qQ/h)S \quad (4)$$

where $e^2qQ/h$ is the quadrupolar coupling constant and $S$ is an order parameter that accounts for molecular motion. In this study a $K$ value of 49 kHz was used, as in a previous study (*11*). This corresponds to $S = 0.875$, which was obtained from the splittings in dry powder samples of the peptides. The splittings were similar for WALP23 and KALP23 at different label positions (data not shown).

Values for $\tau$, $\rho$, and $\epsilon_{\parallel}$ were calculated to minimize the error function

$$\text{error} = \sum_n [\Delta\nu_{q,n}{}^{\text{exptl}} - \Delta\nu_{q,n}{}^{\text{calc}}(\tau,\rho,\epsilon_{\parallel})]^2 \quad (5)$$

where the sum is over all labeled positions denoted by the index $n$ in analogy to the $n$ value for $\varphi$ (of eq 3). Angles were varied in steps of 0.1° in the range 0−45° and 51−64° for $\tau$ and $\epsilon_{\parallel}$ (see modeling below), respectively. $\rho$ was varied in the range 0−360° in steps of 1°. The error values for the best fits are presented as root mean square deviations (RMSD). This is defined here as RMSD = (error/number of data points)$^{1/2}$. An in-house computer program written in Python 2.3 was designed to select the best fit values of $\tau$, $\rho$, and $\epsilon_{\parallel}$ corresponding to the lowest RMSD.

*Error Estimates in Fitting.* The maximum deviation for the best fit was evaluated by implementing the error of measurement in the calculations. This error is estimated to be 0.5 kHz on the basis of duplicate measurements or duplicate samples. Calculations were performed with data set combinations of the average values of WALP23 for eight labeled positions in di-12:0-PC from previous work (*14*) ± the error. The data from the four labeled positions in our work were similar to those of the previous study. In that way for each peptide three experimental data were assigned according to

$$\Delta\nu_{q,n} = \Delta\nu_{q,n,\text{experimental}} + 0.5m \quad (6)$$

where $n$ is the residue number and $m$ can be either $-1$, 0, or $+1$ for an error of $-0.5$, 0, and 0.5 kHz, respectively. In that way, $3^n$ data sets were fitted to determine the maximal deviation inherent to this method. The maximal deviations thus calculated were $\pm0.4°$, $\pm3°$, and $\pm0.3°$ for the tilt angle $\tau$, the rotation angle $\rho$, and $\epsilon_{\parallel}$, respectively.

*Analysis of the Relationship between $\epsilon_{\parallel}$ Values and Hydrophobic Length of WALP23 Based on Molecular Modeling.* To determine a realistic range of $\epsilon_{\parallel}$ values for calculation on a transmembrane peptide model, WALP23 has been modeled on the basis of typical parameters of crystal structures of transmembrane helices (*22*). The modeling was performed in DeepView/Swiss-PdbViewer, generating PDB structures by varying the $\phi$ and $\psi$ Ramachandran parameters. To encompass the values of the so-called membrane coils, the α-helical parameters were allowed to vary by steps of 0.5° around the average values of $-64.5° \pm 8.5°$ and $-41°$ $\pm 9.5°$ for $\phi$ and $\psi$, respectively. $\epsilon_{\parallel}$ values of all the generated structures were calculated using a program written in Python 2.3 (kindly provided by Aalt-Jan van Dijk). The range of $\epsilon_{\parallel}$ values was calculated to be between 51° and 64°. The distance between both C$^{\alpha}$ of the outer leucines of all these structures was monitored under DeepView/Swiss-PdbViewer.
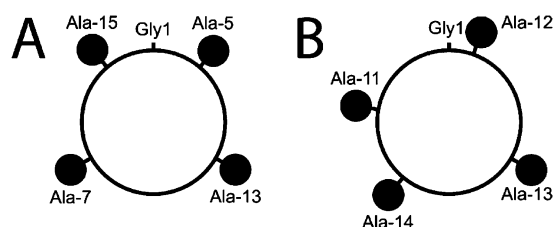
FIGURE 2: Top view from the N-terminus of the helical wheel showing the $d_4$-Ala labeling positions in WALP23 and KALP23 (A) and in WLP23 and KLP23 (B) as indicated by circles.
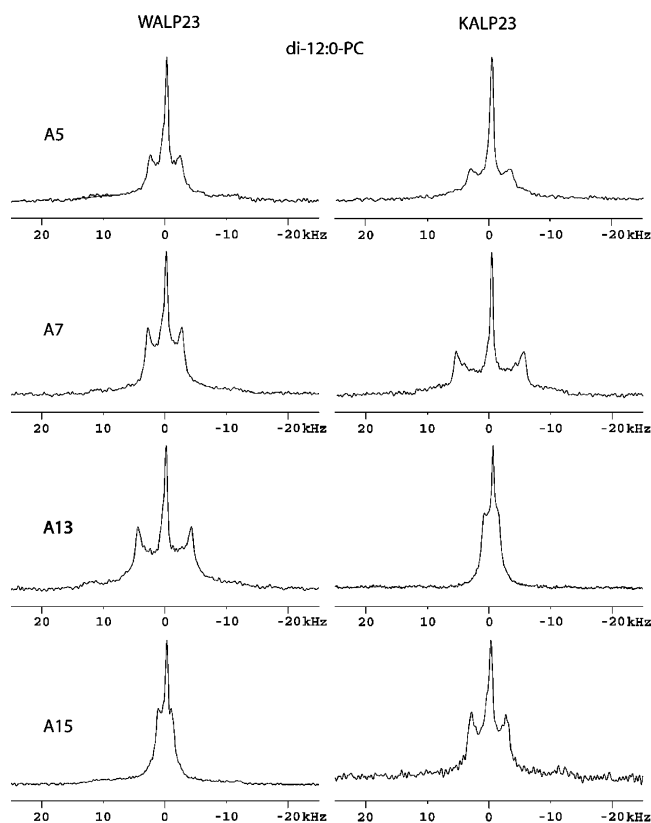


FIGURE 3: $^2$H NMR spectra for labeled alanines at positions 5, 7, 13 and 15 in WALP23 (left panel) and in KALP23 (right panel) incorporated in bilayers of di-12:0-PC at a peptide to lipid molar ratio of 1/100. The labels on the left indicate the position of the $d_4$-labeled alanine along the peptide sequence. The isotropic peak in the middle of the spectra is assigned to residual deuterium in H$_2$O.

$\epsilon_{\parallel}$ values were plotted versus peptide lengths of corresponding structures to determine the relationship between both parameters.

## RESULTS

*Influence of Flanking Residues on Tilt and Rotation Angles.* WALP23 and KALP23 were labeled with a single $d_4$-Ala at four different positions as indicated in Table 1 for each peptide. The choice of labeling position was such to have a homogeneous distribution around the helical wheel (Figure 2A). Figure 3 shows $^2$H NMR spectra of the four different WALP23 and KALP23 peptides in unoriented samples of di-12:0-PC. For both types of peptides defined quadrupolar splittings can be observed, the magnitude of which varies with the position of the label. Also in di-13:0-PC, di-14:0-PC, and di-18:1-PC bilayers a label position-dependent variation of quadrupolar splittings was

Table 2: Measured $^2$H NMR Splittings of $d_4$-Ala-Labeled WALP23 (A) and KALP23 (B) Peptides in Unoriented PC Bilayers in kHz

| phospholipid | peptide | labeled residue | | | |
|---|---|---|---|---|---|
| | | 5 | 7 | 13 | 15 |
| | | Part A | | | |
| di-12:0-PC | WALP23[a] | 4.75 | 5.5 | 8.65 | 2.05 |
| di-13:0-PC | WALP23[a] | 5.3 | 3.5 | 8.7 | 1.65 |
| di-14:0-PC | WALP23[a] | 4.7 | 0.5[b] | 7.75 | 0.5[b] |
| di-18:1-PC | WALP23[a] | 4.7 | 0.35[b] | 6.7 | 0.5[b] |
| | | Part B | | | |
| di-12:0-PC | KALP23 | 6.6 | 11.4 | 1.9 | 5.6 |
| di-13:0-PC | KALP23 | 4.45 | 10.3 | 1.3 | 4.6 |
| di-14:0-PC | KALP23 | 3 | 9.7 | 0[b] | 3.9 |
| di-18:1-PC | KALP23 | 0.2 | 7.9 | 1.9 | 3.1 |

[a] Data as in ref *14*. [b] Splittings that could not be resolved and for which an estimated value is given.

Table 3: Fit Results Using Data from the Four Labeled Positions Summarized in Table 2 for WALP23 (A) and KALP23 (B)

| phospholipid | peptide | tilt angle | rotation angle | CD$_3$ angle | RMSD (kHz) |
|---|---|---|---|---|---|
| | | Part A | | | |
| di-12:0-PC | WALP23 | 8.1 | 134 | 56.5 | 2.2 |
| di-13:0-PC | WALP23 | 7.5 | 139 | 57.4 | 1.3 |
| di-14:0-PC | WALP23 | 5.2 | 155 | 58.5 | 0.3 |
| di-18:1-PC | WALP23 | 4.8 | 146 | 57.9 | 0.13 |
| | | Part B | | | |
| di-12:0-PC | KALP23 | 11.2 | 286 | 58.0 | 0.2 |
| di-13:0-PC | KALP23 | 9 | 286 | 58.0 | 0.5 |
| di-14:0-PC | KALP23 | 7.6 | 281 | 58.3 | 0.8 |
| di-18:1-PC | KALP23 | 4.8 | 273 | 58.8 | 0.9 |

observed, as quantified in Table 2. If one assumes that the peptides adopt a regular α-helical structure, then the observation of a position-dependent variation of $\Delta\nu_q$ implies that both the WALP23 and KALP23 peptides are tilted and that they do not rotate fast around their own axis because otherwise all values of $\Delta\nu_q$ would have been similar. Measurements on oriented samples for the four types of peptides showed that instead the peptides undergo fast reorientation about the bilayer normal, in agreement with earlier studies on these and similar peptides (*10*, *11*, *14*).

Table 2 shows that for almost all labeled positions systematic changes in quadrupolar splitting occur, whereby the quadrupolar splitting decreases with increasing bilayer thickness from di-12:0-PC to di-18:1-PC. From the quadrupolar splittings obtained for the different labeled positions, tilt and rotation angles were calculated on the basis of an α-helical geometry of the peptides and on a geometric analysis of labeled alanine (GALA) (*14*). The results are shown in Table 3. When the acyl chain length is increased, the calculated tilt angle of both peptides decreases, suggesting that the changes in tilt angle are a response to hydrophobic mismatch. For WALP23 the tilt angle varies from 8.2° to 4.4° with increasing hydrophobic thickness of the membrane, and the tilt angle of KALP23 changes from 11.2° to 4.8°. Although the calculated tilt angles are quite small, KALP23 tilts significantly more than WALP23 in the thinner membranes.

In contrast to the tilt angles, the rotation angles of both WALP23 and KALP23 are relatively independent of the type of phospholipid bilayer (Table 3). The rotation of Gly1 in WALP23 around the helical axis has an angle between 134°
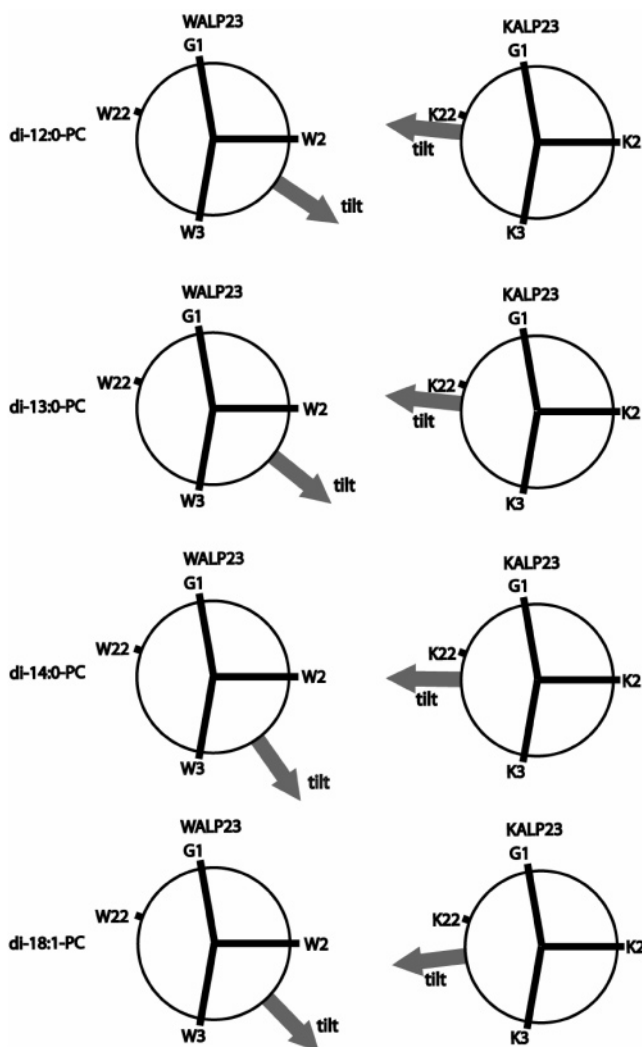
FIGURE 4: View of the helical wheel for WALP23 (left column) and KALP23 (right column) from the N-terminal side with the direction of the tilt indicated with respect to the Gly1 residue, representing the rotation angle. The orientation of tryptophans and lysines at positions 2, 3, and 22 are indicated. From top to bottom, results in di-12:0-PC, di-13:0-PC, di-14:0-PC, and di-18:1-PC are presented.

and 155° with respect to the direction of the tilt, whereas the range of the rotation angles of KALP23 lies between 273° and 286°. The rotation angles are defined by the direction of the tilt as is depicted in Figure 4. This figure shows that WALP23 and KALP23 are tilted in a completely different direction when compared to each other, suggesting a strong influence of the flanking residues in orienting the peptides in membranes.

Table 3 also shows the values used for the side chain angles of the deuterated alanine ($\epsilon_{\parallel}$) to obtain the best fit. Values for WALP23 seem to increase slightly with increasing bilayer thickness for di-12:0-PC, di-13:0-PC, and di-14:0-PC, while for KALP23 such dependence is less evident. This may suggest small adaptations of backbone structure for WALP peptides under conditions of positive mismatch.

Root mean square deviation (RMSD) values are also summarized in Table 3 as an indication of quality of the fits. RMSD values of WALP23 increase with thinner bilayers as observed previously (*14*). In the case of KALP23, RMSD values are rather small for all bilayer thicknesses, indicating a good fit.
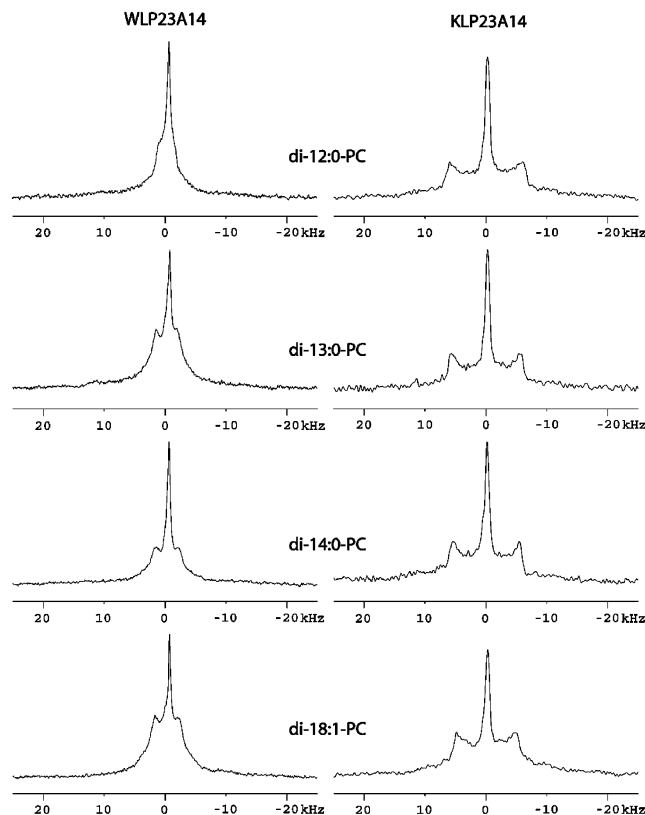


FIGURE 5: $^2$H NMR spectra for WLP23 (left panel) and KLP23 (right panel) labeled at position 14 and incorporated in bilayers of di-12:0-PC, di-13:0-PC, di-14:0-PC, and di-18:1-PC (from top to bottom).

*Effects of Peptide Hydrophobicity on Tilt and Rotation Angles.* Next, we investigated the effect of hydrophobicity by changing the leucine alanine repeat (poly-LA) of the hydrophobic central core of the peptides for polyleucine stretches (poly-L), in which a $d_4$-Ala label was incorporated at a suitable position (Table 1). For each peptide the choice of labeling position was such that a homogeneous distribution around the helical wheel is obtained (Figure 2B) and that a relatively symmetrical distribution of the hydrophobicity along the central poly-L stretch is ensured. Measurements were performed for each peptide in di-12:0-PC, di-13:0-PC, di-14:0-PC, and di-18:1-PC. Figure 5 shows selected $^2$H NMR spectra of $d_4$-Ala14-labeled peptides in the different lipid systems. The quadrupolar splitting varies with hydrophobic thickness of the membrane for both Trp- and Lys-flanked peptides, as quantified in Table 4 for all labeled positions. As is the case for WALP23 and KALP23, WLP23 and KLP23 had different $\Delta\nu_q$ values depending on the position of the label, indicating that the peptides are tilted in the membrane and that they do not rotate fast around their own axis. Calculations based on an α-helical geometry of the peptides are summarized in Table 5. When the acyl chain length is increased, the calculated tilt angle of both peptides decreases, consistent with a response to hydrophobic mismatch. The tilt angles vary from 11.4° to 4.5° for WLP23 and from 10.6° to 6.4° for KLP23. Comparison of tilt angles between WALP23 and WLP23 shows that the substitution of poly-LA by poly-L produces considerably larger tilt angles in the thinner bilayers (Tables 3A and 5A). Their Lys-flanked counterparts, KALP23 and KLP23, show more similar tilting behavior when compared to each other (Tables 3B and 5B).

Table 4:  Measured $^2$H NMR Splittings of $d_4$-Ala-Labeled WLP23 (A) and KLP23 (B) Peptides in Unoriented PC Bilayers in kHz

| phospholipid | peptide | labeled residue | | | |
|---|---|---|---|---|---|
| | | 11 | 12 | 13 | 14 |
| | | Part A | | | |
| di-12:0-PC | WLP23 | 7.3 | 1.6 | 10.5 | 2.4 |
| di-13:0-PC | WLP23 | 4.1 | 1.4 | 10.0 | 3.1 |
| di-14:0-PC | WLP23 | 2.7 | 1.2 | 9.6 | 4.4 |
| di-18:1-PC | WLP23 | 1 | 2.5 | 7.7 | 4.6 |
| | | Part B | | | |
| di-12:0-PC | KLP23 | 7.9 | 5.3 | 1.3 | 12.0 |
| di-13:0-PC | KLP23 | 7.6 | 4.0 | 2.2 | 11.3 |
| di-14:0-PC | KLP23 | 7.3 | 2.7 | 2.6 | 10.9 |
| di-18:1-PC | KLP23 | 6.6 | 0.85 | 3.1 | 9.8 |

Table 5:  Fit Results Using Data from All Labeled Positions for WLP23 (A) and KLP23 (B)

| phospholipid | peptide | tilt angle | rotation angle | CD$_3$ angle | RMSD (kHz) |
|---|---|---|---|---|---|
| | | Part A | | | |
| di-12:0-PC | WLP23 | 11.4 | 175 | 56.5 | 0.1 |
| di-13:0-PC | WLP23 | 8.9 | 170 | 58.3 | 0.2 |
| di-14:0-PC | WLP23 | 8.1 | 176 | 58.7 | 0.4 |
| di-18:1-PC | WLP23 | 4.5 | 179 | 59.4 | 0.1 |
| | | Part B | | | |
| di-12:0-PC | KLP23 | 10.6 | 267 | 58.4 | 0.9 |
| di-13:0-PC | KLP23 | 9.4 | 265 | 58.9 | 0.6 |
| di-14:0-PC | KLP23 | 8.3 | 265 | 59.3 | 0.7 |
| di-18:1-PC | KLP23 | 6.4 | 265 | 59.5 | 0.8 |

As in the poly-LA analogues the rotation angles of WLP23 and KLP23 are very different and appear to be independent of hydrophobic mismatch. Directions of tilt of these peptides are illustrated in Figure 6. Comparison of the rotation angles of WLP23 and KLP23 to those of their respective poly-LA counterparts shows that the direction of the tilt is hardly influenced by the hydrophobicity of the central stretch (Tables 3 and 5). Instead, the rotation angles seemed to be determined almost exclusively by the flanking residues.

Comparison of the $\epsilon_{\parallel}$ values of WLP23 and KLP23 shows again somewhat larger fluctuations for the Trp-flanked peptide than for the Lys-flanked one, similar to that for the poly-LA analogues WALP23 and KALP23. RMSD values for both poly-L analogues were small, indicating a good quality of the fit even in 12:0-PC under the largest mismatch conditions.

## DISCUSSION

In this study, we have investigated the importance of flanking residues and hydrophobicity of transmembrane peptides for influencing tilt and rotation angles in lipid bilayers as a function of bilayer thickness. For this, we have used solid-state deuterium NMR on isotopically labeled transmembrane peptides analogous to WALP23. Our approach is based on GALA, a recently developed method (11) to study tilt and rotation angles that can only be applied on transmembrane peptides when they have a more or less regular α-helical structure. Indeed, circular dichroism spectra showed patterns that were typical of α-helical structures for all studied peptides in small unilamellar vesicles made of di-12:0-PC and di-18:1-PC at a peptide to lipid molar ratio of 1/100 (data not shown). The spectra were similar to those previously reported for WALP23 and KALP23 in di-14:0-PC bilayers (19).
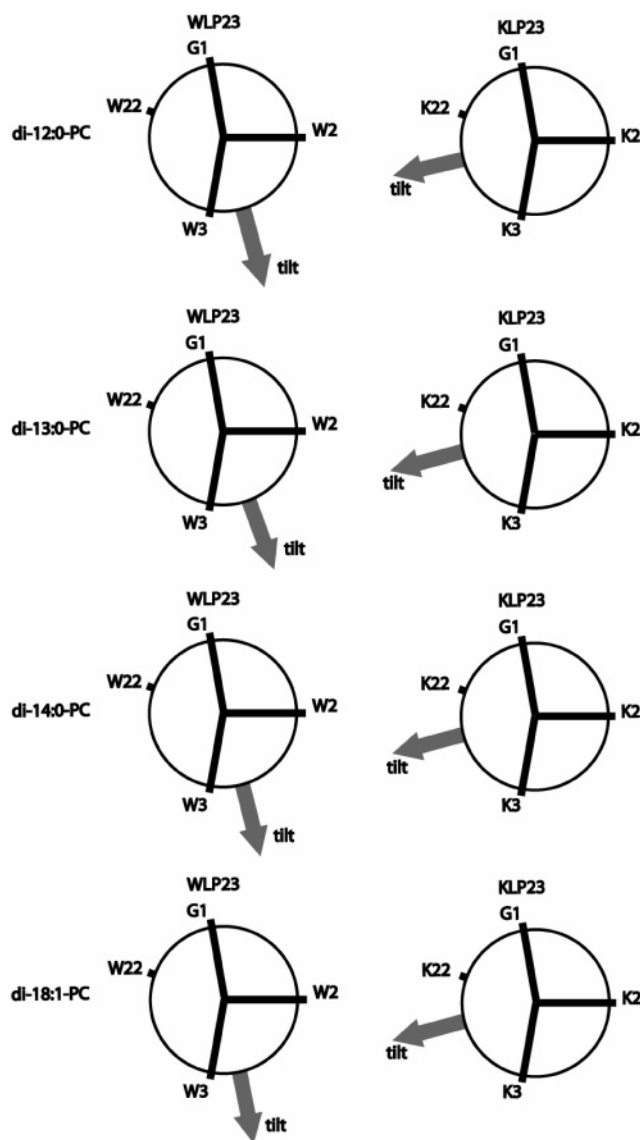


FIGURE 6:  View of the helical wheel for WLP23 (left column) and KLP23 (right column) from the N-terminal side with the direction of the tilt indicated with respect to the Gly1 residue, representing the rotation angle. The rotation of tryptophans and lysines at positions 2, 3, and 22 are indicated. From top to bottom, results in di-12:0-PC, di-13:0-PC, di-14:0-PC, and di-18:1-PC are presented.

The regular α-helical character of the peptides is particularly important for the use of GALA if a limited number of data points are available. GALA has been recently applied to WALP23 in similar PC-bilayers as in this work using singly labeled peptides with deuterated alanine at eight different positions, hence using eight data points (14). That study showed that the method is applicable to a minimum of four data points, whereby the quality of the fit as reflected by the RMSD values may decrease when there are local distortions from the regular α-helical geometry. In the present study, the RMSD values are generally low, indicating that there is no significant distortion from a regular α-helical structure (Tables 3 and 5), and the fit parameters could be determined with high precision. The maximal errors in fit parameters for all samples were estimated to be very low: ±0.4°, ±3°, and ±0.3° for the tilt angle τ, the rotation angle ρ, and $\epsilon_{\parallel}$, respectively (see Materials and Methods). This allows us to differentiate between very small variations in fit parameters that reflect subtle changes in lipid−peptide

interactions. We will now discuss how flanking residues and hydrophobicity when analyzed as a function of hydrophobic mismatch can modulate tilt, rotation, and backbone structure.

*Tilt Angles.* When the hydrophobic length of a transmembrane peptide exceeds the hydrophobic thickness of a bilayer, it may be expected to tilt. Recently, the tilt angles of WALP23 were analyzed in bilayers of different thickness (*14*). A small nonzero tilt angle was obtained in the absence of hydrophobic mismatch. This was also observed for the shorter WALP19 (*11*). Here we show that when the tryptophan residues in WALP23 are replaced by lysines (KALP23), a similar nonzero tilt angle is adopted in di-18:1-PC bilayers (Table 3). These results suggest that a small nonzero tilt under matching conditions can be an intrinsic property of transmembrane peptides, which may be attributed to a nonsymmetrical distribution of the amino acids along the helical axis.

When the bilayer thickness was decreased, both WALP23 and KALP23 showed a small but systematic increase in tilt angle in response to positive hydrophobic mismatch. However, the tilt angle of KALP23 showed a significantly larger mismatch sensitivity. KALP23 tilt angles varied from about 5° to 11° with decreasing bilayer thickness, while tilt angles of WALP23 varied from about 4° to 8° (Table 3). The 3° difference in tilt between the two peptides in the thinnest bilayers is likely to be effectively larger, because the effective hydrophobic length of KALP23 is smaller than that of WALP23 due to the more hydrophobic character of Trp residues and their preferred positioning near the interface (*19*, *23*). The relatively weak sensitivity to mismatch for WALP23 suggests that, under positive mismatch conditions, Trp residues may inhibit tilting of transmembrane segments of membrane proteins. The reason for this is not known, but one might speculate that the preferred positioning of Trp at the interface (*24*) in combination with distinct, energetically favored torsion angles of the side chain may render tilt unfavorable.

The main reason for a transmembrane peptide to tilt in response to hydrophobic mismatch is to limit the energetic penalty due to exposure of its hydrophobic regions to a polar interfacial environment. Enhancing the hydrophobicity of the transmembrane part may be expected to increase this penalty, hence to increase the tilt angle. Our results showed that in the matching di-18:1-PC bilayer the tilt angle of WLP23 is similar to the one of WALP23 but that when positive mismatch is achieved by using shorter phospholipids, the tilt angle of WLP23 indeed becomes systematically larger than for WALP23. In contrast, hydrophobicity did not seem to significantly affect the tilt of Lys-flanked peptides. The maximum tilt angles for both peptides are around 11° in a di-12:0-PC membrane, similar to the maximum tilt angle of WLP23. These tilt angles are small considering the fact that a tilt angle of about 40° would be required to fully match the hydrophobic thickness by tilting (*14*). Together, the results suggest that the energy barrier for adopting tilt angles above 11−12° is rather high. One might speculate that this energy barrier is related to packing properties of the lipids. The insertion of a transmembrane peptide with a large tilt angle would severely perturb the packing of the lipids surrounding the peptide, which in turn would perturb lipid−lipid interactions with neighboring lipids.

The results obtained for KALP can be compared with literature data that are available on other Lys-flanked peptides in slightly different peptide−lipid systems. Using solid-state NMR on Lys-flanked peptides with deuterated alanines, but using fewer label positions, Sharpe and co-workers also reported a relatively small tilt angle in bilayers of 16:0/18:1_c-PC (*10*) for a peptide with the same hydrophobic length as KALP23, while a slightly larger tilt angle was observed for a five amino acid longer peptide, in agreement with the mismatch dependence of the results presented here. Our results are also consistent with tilt angles determined from ^{15}N NMR on Lys-flanked peptides of varying length in unsaturated bilayers of varying thickness (*7*). Although the precise tilt angle could not be determined in these samples, because the rotation angle was not known, the minimum values obtained for the tilt angles in this study were close to the values obtained in our study.

*Rotation Angles.* When a transmembrane peptide is tilted in a bilayer and it is not rotating around its long axis, it has a preferential direction of tilt with respect to the membrane. This rotation angle is another important determinant for lipid−peptide interactions.

The rotation angles of WALP23 and KALP23 are rather constant in the studied bilayers, suggesting that the direction of the tilt is independent of hydrophobic mismatch. Interestingly, comparison of the rotation angles of WALP23 and KALP23 shows that they differ from each other. This demonstrates that lipid-peptide interactions at the membrane−water interface play a dominant role in determining the direction in which a peptide is tilted in a membrane. This is further supported by the observation that also the hydrophobicity does not significantly affect the rotation angle. Although rotation angles of transmembrane segments of proteins have been determined before by solid-state NMR techniques (*25*, *26*), to our knowledge this is the first time that parameters that determine rotation angles have been investigated.

*Effects of Flanking Residues on the Backbone Structure.* As mentioned earlier, the fit procedure includes a value of $\epsilon_{\parallel}$, which is the side chain angle of the deuterated alanine with respect to the helix axis. The results suggest that the $\epsilon_{\parallel}$ values of Trp-flanked peptides may be more sensitive to bilayer thickness than those of their Lys analogues. When a grid of α-helical structures is produced, as described in Materials and Methods, using any realistic $\phi$ and $\psi$ Ramachandran parameters, and $\epsilon_{\parallel}$ values of these structures are plotted against the calculated distance between the outer $C_{\alpha}$ carbons of the outer leucines in the sequence, a nearly linear relationship is obtained (Figure 7). From this relationship it can be estimated that WALP23 and WLP23 in di-12:0-PC correspond to structures that have a slightly shorter hydrophobic length (up to 1.8 Å) than their Lys-flanked counterparts. This suggests that the anchoring of the tryptophan residues to the membrane−water interface may cause the peptides to help to adapt to mismatch by slightly reducing their length in addition to tilting.

Such small adaptations of peptide length were not measurable by ATR-FTIR in very similar peptide−lipid systems (*27*), which illustrates the exceptional sensitivity of the GALA method to very small changes in backbone structure. The observation of small changes in backbone structure for Trp-flanked peptides but not for Lys-flanked peptides is
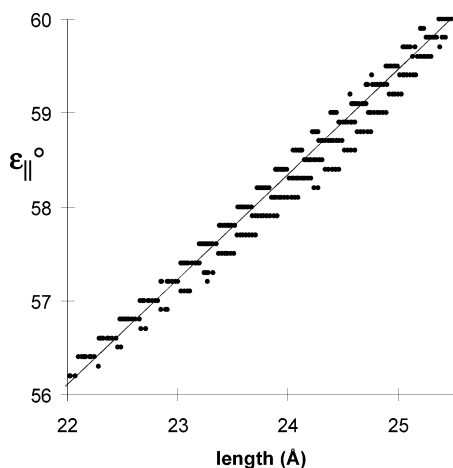
FIGURE 7: Relation between the alanine side chain angle with respect to the helix axis ($\epsilon_{\parallel}$) and the length of α-helical structures, calculated as the distance in Å between the $C^\alpha$ of the outer leucines, as described in the Materials and Methods section. Dots represent calculated values, and the straight line represents a regression line. Only the range that encompasses the experimental $\epsilon_{\parallel}$ values as listed in Tables 3 and 5 is represented.

consistent with the postulated strong interaction of Trp with the interface (*24*). Interestingly, from this strong interaction one would predict more tilting of the WALP23 peptide in response to mismatch as compared to KALP23, instead of inhibition of the tilt, as we observed. We propose that the preferred positioning of Trp at the interface (*24*) in combination with distinct, energetically favored torsion angles of the side chain may render tilt of transmembrane segments with Trp as flanking residues less sensitive to positive mismatch and that instead other responses are favored, such as adaptation of the peptide backbone and ordering and stretching of the lipid chains (*24*).

*Implications for Membrane Proteins.* In this study we have determined both tilt and rotation angles of α-helical transmembrane segments in different peptide−lipid model systems with high accuracy. Rather surprisingly, in all peptides we observed only very small changes in peptide tilt and rotation as a function of lipid length. Nevertheless, in biological membranes such subtle changes may be important because they can be sufficient for modulating activity of membrane proteins. Examples of proteins that require only small structural changes for activity are bacteriorhodopsin upon transition to an intermediate state of its photocycle (*28*) and the rhodopsin II−transducer complex, in which light activation may trigger a signal cascade by inducing a small tilt movement, which in turn initiates a rotation of transmembrane helices (*29*; reviewed in ref *30*).

In contrast to the relatively small effect of lipid length, we observed large effects when the flanking Trp residues were replaced by Lys, including a significant increase in the extent of tilting, and a completely different direction of tilt, or rotation angle. These results may be important to help in understanding and predicting the precise arrangement of transmembrane segments of membrane proteins in lipid bilayers and how this arrangement can be modulated by interactions with surrounding lipids. An interesting example is the mechanosensitive channel MscL, which experiences conformational changes involving large tilt and twist rotation motions of its transmembrane regions upon changes in membrane tension (*31*, *32*). MscL is one of the few

membrane proteins of which the transmembrane segments are not enriched in aromatic amino acids as flanking residues, and it was recently shown that introduction of Trp or Tyr at these positions can result in loss of functionality of the protein (*33*). Our observations that Trp seems to inhibit tilting of transmembrane segments and that the flanking residues are important for determining the rotation angle provide a plausible explanation for this effect.

## ACKNOWLEDGMENT

## REFERENCES

1. Lee, A. G. (2003) Lipid−protein interactions in biological membranes: a structural perspective, *Biochim. Biophys. Acta 1612*, 1−40.
2. Killian, J. A. (1998) Hydrophobic mismatch between proteins and lipids in membranes, *Biochim. Biophys. Acta 1376*, 401−416.
3. Dumas, F., Lebrun, M. C., and Tocanne, J. F. (1999) Is the protein/lipid hydrophobic matching principle relevant to membrane organization and functions?, *FEBS Lett. 458*, 271−277.
4. de Planque, M. R. R., and Killian, J. A. (2003) Protein−lipid interactions studied with designed transmembrane peptides: role of hydrophobic matching and interfacial anchoring, *Mol. Membr. Biol. 20*, 271−284.
5. Huschilt, J. C., Millman, B. M., and Davis, J. H. (1989) Orientation of α-helical peptides in a lipid bilayer, *Biochim. Biophys. Acta 979*, 139−141.
6. Killian, J. A., Salemink, I., de Planque, M. R. R., Lindblom, G., Koeppe, R. E., II, and Greathouse, D. V. (1996) Induction of nonbilayer transmembrane α-helical peptides: importance of hydrophobic mismatch and proposed role of tryptophans, *Biochemistry 35*, 1037−1045.
7. Harzer, U., and Bechinger, B. (2000) Alignment of lysine-anchored membrane peptides under conditions of hydrophobic mismatch: A CD, $^{15}$N and $^{31}$P solid-state NMR spectroscopy investigation, *Biochemistry 39*, 13106−13114.
8. Liu, F., Lewis, R. N., Hodges, R. S., and McElhaney, R. N. (2001) A differential scanning calorimetric and $^{31}$P NMR spectroscopic study of the effect of transmembrane α-helical peptides on the lamellar-reversed hexagonal phase transition of phosphatidylethanolamine model membranes, *Biochemistry 40*, 760−768.
9. Mall, S., Broadbridge, R., Sharma, R. P., East, J. M., and Lee, A. G. (2001) Self-association of model transmembrane α-helices is modulated by lipid structure, *Biochemistry 40*, 12379−12386.
10. Sharpe, S., Barber, K. R., Grant, C. W., Goodyear, D., and Morrow, M. R. (2002) Organization of model helical peptides in lipid bilayers: insight into the behavior of single-span protein transmembrane domains, *Biophys. J. 83*, 345−358.
11. Van der Wel, P. C. A., Strandberg, E., Killian, J. A., and Koeppe, R. E., II (2002) Geometry and intrinsic tilt of a tryptophan-anchored transmembrane α-helix determined by $^2$H NMR, *Biophys. J. 83*, 1479−1488.
12. Caputo, G. A., and London, E. (2003) Cumulative effects of amino acid substitutions and hydrophobic mismatch upon the transmembrane stability and conformation of hydrophobic α-helices, *Biochemistry 42*, 3275−3285.
13. Subczynski, W. K., Pasenkiewicz-Gierula, M., McElhaney, R. N., Hyde, J. S., and Kusumi, A. (2003) Molecular dynamics of 1-palmitoyl-2-oleoylphosphatidylcholine membranes containing transmembrane α-helical peptides with alternating leucine and alanine residues, *Biochemistry 42*, 3939−3948.
14. Strandberg, E., Özdirekcan, S., Rijkers, D. T. S., van der Wel, P. C. A., Koeppe, R. E., II, Liskamp, R. M. J., and Killian, J. A. (2004) Tilt angles of transmembrane model peptides in oriented and nonoriented lipid bilayers as determined by $^2$H solid-state NMR, *Biophys. J. 86*, 3709−3721.
15. Killian, J. A. (2003) Synthetic peptides as models for intrinsic membrane proteins, *FEBS Lett. 555*, 134−138.

16. Jones, D. H., Barber, K. R., VanDerLoo, E. W., and Grant, C. W. M. (1998) Epidermal growth factor receptor transmembrane domain: $^2$H NMR implications for orientation and motion in a bilayer environment, *Biochemistry 37*, 16780−16787.

17. Yau, W. -M., Wimley, W. C., Gawrisch, K., and White, S. H. (1998) The preference of tryptophan for membrane interfaces, *Biochemistry 37*, 14713−14718.

18. Persson, S., Killian, J. A., and Lindblom, G. (1998) Molecular ordering of interfacially localized tryptophan analogues in ester- and ether-lipid bilayers studied by $^2$H NMR, *Biophys. J. 75*, 1365−1371.

19. de Planque, M. R. R., Kruijtzer, J. A. W., Liskamp, R. M. J., Marsh, D., Greathouse, D. V., Koeppe, R. E., II, de Kruijff, B., and Killian, J. A. (1999) Different membrane anchoring positions of tryptophan and lysine in synthetic transmembrane α-helical peptides, *J. Biol. Chem. 274*, 20839−20846.

20. Ten Kortenaar, P. B. W., van Dijk, B. G., Peters, J. M., Raaben, B. J., Adams, P. J. H. M., and Tesser, G. I. (1986) Rapid and efficient method for the preparation of Fmoc-amino acids starting from 9-fluorenylmethanol, *Int. J. Pept. Protein Res. 27*, 398−400.

21. Rouser, G., Fleisher, S., and Yamamoto, A. (1970) Two-dimensional thin layer chromatographic separation of polar lipids and determination of phospholipids by phosphorus analysis of spots, *Lipids 5*, 494−496.

22. Hildebrand, P. W., Preissner, R., and Frömmel, C. (2004) Structural features of transmembrane helices, *FEBS Lett. 559*, 145−151.

23. Strandberg, E., Morein, S., Rijkers, D. T. S., Liskamp, R. M. J., van der Wel, P. C. A., and Killian, J. A. (2002) Lipid dependence of membrane anchoring properties and snorkeling behavior of aromatic and charged residues in transmembrane peptides, *Biochemistry 41*, 7190−7198.

24. de Planque, M. R. R., Bonev, B. B., Demmers, J. A. A., Greathouse, D. V., Koeppe, R. E., II, Separovic, F., Watts, A., and Killian, J. A. (2003) Interfacial anchor properties of tryptophan residues in transmembrane peptides can dominate over hydro-phobic matching effects in peptide-lipid interactions, *Biochemistry 42*, 5341−5348.

25. Marassi, F. M., and Opella, S. J. (2000) A solid-state NMR index of helical membrane protein structure and topology, *J. Magn. Reson. 144*, 150−155.

26. Kovacs, F. A., Denny, J. K., Song, Z., Quine, J. R., and Cross, T. A. (2000) Helix tilt of the M2 transmembrane peptide from influenza A virus: An intrinsic property, *J. Mol. Biol. 295*, 117−125.

27. de Planque, M. R. R., Goormaghtigh, E., Greathouse, D. V., Koeppe, R. E., II, Kruijtzer, J. A. W., Liskamp, R. M. J., de Kruijff, B., and Killian, J. A. (2001) Sensitivity of single membrane-spanning α-helical peptides to hydrophobic mismatch with a lipid bilayer: effects on backbone structure, orientation, and extent of membrane incorporation, *Biochemistry 40*, 5000−5010.

28. Dencher, N. A., Dresselhaus, D., Zaccaï, G., and Büldt, G. (1989) Structural changes in bacteriorhodopsin during proton translocation revealed by neutron diffraction, *Proc. Natl. Acad. Sci. U.S.A. 86*, 7876−7879.

29. Wegener, A. A., Klare, J. P., Engelhard, M., and Steinhoff, H. J. (2001) Structural insights into the early steps of receptor-transducer signal transfer in archaeal phototaxis, *EMBO J. 20*, 5312−5319.

30. Klare, J. P., Gordeliy, V. I., Labahn, J., Büldt, G., Steinhoff, H.-J., and Engelhard, M. (2004) The archaeal sensory rhodopsin II/transducer complex: a model for transmembrane signal transfer, *FEBS Lett. 564*, 219−222.

31. Sukharev, S., Durell, S. R., and Guy, H. R. (2001) Structural models of the MscL gating mechanism, *Biophys. J. 81*, 917−936.

32. Valadié, H., Lacapcre, J. J., Sanejouand, Y.-H., and Etchebest, C. (2003) *J. Mol. Biol. 332*, 657−674.

33. Chiang, C. S. Shirinian, L. A., and Sukharev, S. (2004) *Biophys. J. 86*, 546A (part 2, Suppl. S).